

Role of the Sterol Carrier Protein-2 N-Terminal Membrane Binding Domain in Sterol Transfer[†]

Huan Huang,[‡] Adalberto M. Gallegos,[‡] Minglong Zhou,[‡] Judith M. Ball,[§] and Friedhelm Schroeder^{*,‡}

Department of Physiology and Pharmacology and Department of Pathobiology, Texas A&M University, TVMC, College Station, Texas 77843

Received May 1, 2002; Revised Manuscript Received August 9, 2002

ABSTRACT: Previous studies showed that the N-terminal 32 amino acids of sterol carrier protein-2 (^{1–32}SCP₂) comprise an amphipathic α -helix essential for SCP₂ binding to membranes [Huang et al. (1999) *Biochemistry* 38, 13231]. However, it is unclear whether membrane interaction of the ^{1–32}SCP₂ portion of SCP₂ is in itself sufficient to mediate intermembrane sterol transfer, possibly by altering membrane structure. In this study a fluorescent sterol exchange assay was used to resolve these issues and demonstrated that the SCP₂ N-terminal peptide ^{1–32}SCP₂ did not by itself enhance intermembrane sterol transfer but potentiated the ability of the SCP₂ protein to stimulate sterol transfer. Compared with SCP₂ acting alone, ^{1–32}SCP₂ potentiated the sterol transfer activity of SCP₂ by increasing the initial rate of sterol transfer by 2.9-fold and by decreasing the half-time of sterol transfer by 10-fold (from 11.6 to 1.2 min) without altering the size of the transferable fractions. The ability of a series of SCP₂ mutant N-terminal peptides to potentiate SCP₂-mediated sterol transfer was directly correlated with membrane affinity of the respective peptide. N-Terminal peptide ^{1–32}SCP₂ did not potentiate intermembrane sterol transfer by binding sterol (dehydroergosterol), altering membrane fluidity (diphenylhexatriene) or membrane permeability (leakage assay). Instead, fluorescence lifetime measurements suggested that SCP₂ and ^{1–32}SCP₂ bound to membranes and thereby elicited a shift in membrane sterol microenvironment to become more polar. In summary, these data for the first time showed that while the N-terminal membrane binding domain of SCP₂ was itself inactive in mediating intermembrane sterol transfer, it nevertheless potentiated the ability of SCP₂ to enhance sterol transfer.

Sterol carrier protein-2 (SCP₂)¹ is a ubiquitous protein highly enriched in tissues active in cholesterol metabolism and steroidogenesis (1). Although much of our early knowledge regarding the function of SCP₂ in intermembrane sterol

transport came from *in vitro* studies with model membranes (2–8), more recent findings indicate that SCP₂ is also highly active in enhancing sterol transfer from biological membranes *in vitro*: plasma membranes (9, 10), lysosomes (11, 12), mitochondria (9, 10, 13), and endoplasmic reticulum (ER) (9, 10, 12). Furthermore, *in vitro* studies with different donor/acceptor membrane pairs (1) as well as experiments with transfected cells (14) suggest that SCP₂-mediated transfer of cholesterol between specific intracellular membranes is vectorial. The level of SCP₂ expression regulates cholesterol uptake (15), cholesterol efflux (14, 16), intracellular cholesterol distribution (1, 12, 14, 17), intracellular cholesterol and cholesteryl ester accumulation (18–20), and biliary cholesterol secretion (21, 22).

The above functions of SCP₂ are consistent with the intracellular localization of SCP₂. Since SCP₂ has a C-terminal peroxisomal targeting sequence, it is not surprising that immunogold electron microscopy and immunofluorescence confocal microscopy detect SCP₂ in highest concentration in peroxisomes, an organelle essential for production of certain bile acids (1, 23, 24). Nevertheless, nearly half of total SCP₂ is extraperoxisomal (1, 13, 23–27). The apparent inconsistency in these observations was recently resolved by the discovery of the role of the N-terminal 20 amino acid presequence present in pro-SCP₂, the precursor coded for by the SCP₂ gene and translated in ER (27). Although SCP₂

[†] This work was supported by USPHS National Institutes of Health Grants GM31651 (F.S.) and GM63236 (J.M.B.).

^{*} To whom correspondence should be addressed. Tel: 979-862-1433. Fax: 979-862-4929. E-mail: fschroeder@cvm.tamu.edu.

[‡] Department of Physiology and Pharmacology, Texas A&M University.

[§] Department of Pathobiology, Texas A&M University.

¹ Abbreviations: SCP₂, sterol carrier protein-2; ^{1–32}SCP₂, Ser-Ser-Ala-Ser-Asp-Gly-Phe-Lys-Ala-Asn-Leu-Val-Phe-Lys-Glu-Ile-Glu-Lys-Lys-Leu-Glu-Glu-Gly-Glu-Gln-Phe-Val-Lys-Lys-Ile-Gly-NH₂; ^{1–24}SCP₂, Ser-Ser-Ala-Ser-Asp-Gly-Phe-Lys-Ala-Asn-Leu-Val-Phe-Lys-Glu-Ile-Glu-Lys-Lys-Leu-Glu-Glu-Gly-NH₂; ^{10–32}SCP₂, Asn-Leu-Val-Phe-Lys-Glu-Ile-Glu-Lys-Lys-Leu-Glu-Glu-Gly-Glu-Gln-Phe-Val-Lys-Lys-Ile-Gly-NH₂; ^{1–E20–32}SCP₂, ^{1–32}SCP₂, Ser-Ser-Ala-Ser-Asp-Gly-Phe-Lys-Ala-Asn-Leu-Val-Phe-Lys-Glu-Ile-Glu-Lys-Lys-Leu-Glu-Glu-Gly-Glu-Gln-Phe-Val-Lys-Lys-Ile-Gly-NH₂; MALDI/TOF, matrix-assisted laser desorption/ionization/time-of-flight mass spectrometry; HPLC, high-performance liquid chromatography; PBS, phosphate-buffered saline; PIPES, piperazine-*N,N'*-bis(2-ethanesulfonic acid); MOPS, 3-(*N*-morpholino)propanesulfonic acid; ANTS, 8-aminonaphthalene-1,3,6-trisulfonic acid disodium salt; DPX, *p*-xylenebis(pyridinium bromide); POPC (also called phosphatidylcholine), 1-palmitoyl-2-oleoyl-*sn*-glycero-3-phosphocholine; DOPS (also called phosphatidylserine), 1,2-dioleoyl-*sn*-glycero-3-phospho-L-serine; DHE, dehydroergosterol; SUV, small unilamellar vesicles; NBD-stearic acid, (7-nitrobenz-2-oxa-1,3-diazolyl)octadecanoic acid; DPH-PC, 2-[3-(diphenylhexatrienyl)propanoyl]-1-hexadecanoyl-*sn*-glycero-3-phosphocholine.

contains a C-terminal peroxisomal targeting sequence, this epitope is poorly exposed at the surface of the SCP₂ protein (27). Furthermore, transfecting cells with the cDNA encoding SCP₂ results in weak targeting of SCP₂ to peroxisomes (27). In contrast, pro-SCP₂ is conformationally altered to expose the C-terminal peroxisomal targeting sequence (27). Consequently, transfecting cells with the cDNA encoding pro-SCP₂ increases the targeting to peroxisomes severalfold to levels accounting for as much as half of total SCP₂ (27). These data suggest that the exact intracellular distribution of SCP₂ within cells will depend not only on the presence of the C-terminal peroxisomal targeting sequence but also on the rate of proteolytic removal of the N-terminal presequence from pro-SCP₂ before and/or after entry into the peroxisome.

Although the structure of SCP₂ has been investigated by fluorescence (28–30), circular dichroism (27, 31–33), and NMR (24, 32, 34–38), only recently was the complete tertiary structure resolved by X-ray crystallography (39, 40). Despite these advances, molecular details regarding the mechanism(s) whereby SCP₂ mediates intermembrane sterol transfer are much less well understood. Two structural features of SCP₂ appear essential for mediating intermembrane sterol transfer: (i) An intact ligand binding site is essential for sterol transfer activity (41). However, the amino acid residues constituting the sterol binding site have to date not been identified. (ii) SCP₂ must interact/bind directly with membranes to mediate intermembrane sterol transfer (41–43). Model membrane studies have shown that SCP₂ binds membranes primarily through ionic interactions between the positively charged face of the N-terminal amphipathic α -helical region of SCP₂ and the negatively charged phospholipids in the membrane surface (42, 43). SCP₂ and its N-terminal peptide ^{1–32}SCP₂ bind to anionic phospholipid-containing small unilamellar vesicle (SUV) membranes and undergo significant alteration in secondary structure (42, 43). The SCP₂ N-terminal peptide ^{1–32}SCP₂, primarily random coil in aqueous buffer, adopts α -helical structure upon interaction with membranes. However, it is not clear whether SCP₂ binding to membranes via this N-terminal ^{1–32}SCP₂ peptide alone is sufficient to elicit intermembrane sterol transfer, possibly by disruption of membrane structure.

The objective of the present investigation was to begin to resolve these issues by (i) determining if a series of SCP₂ N-terminal peptides by themselves enhance intermembrane sterol transfer, (ii) resolving whether SCP₂ N-terminal peptides compete with SCP₂ to inhibit sterol transfer or, alternately, facilitate/potentiate SCP₂-mediated sterol exchange between membranes, (iii) examining if the effect of SCP₂ N-terminal peptides on SCP₂-mediated sterol exchange correlates with the affinity of the peptides for membrane binding, and (iv) addressing whether SCP₂ and its N-terminal peptides disrupt membrane structure, e.g., permeability and fluidity.

EXPERIMENTAL PROCEDURES

Materials. Human recombinant SCP₂ was prepared as described earlier (44). 1-Palmitoyl-2-oleoyl-*sn*-glycero-3-phosphocholine (POPC) and 1,2-dioleoyl-*sn*-glycero-3-phospho-L-serine (DOPS) were purchased from Avanti Polar

Lipids (Alabaster, AL). Cholesterol, dehydroergosterol, *o*-phthaldialdehyde, trifluoroethanol, β -mercaptoethanol, melittin (approximately 93% HPLC), Sephadex G-50 for gel filtration, and piperazine-*N,N'*-bis(2-ethanesulfonic acid) (PIPES) were purchased from Sigma Chemical Co. (St. Louis, MO). 8-Aminonaphthalene-1,3,6-trisulfonic acid disodium salt (ANTS) and *p*-xylenebis(pyridinium bromide) (DPX) were purchased from Molecular Probes Inc. (Eugene, OR).

Synthesis of Peptides. The peptides were synthesized using a Millipore 9050 Plus (Perceptive Biosystems) automated peptide synthesizer and fluorenylmethoxycarbonyl (Fmoc) solid-phase chemistry (Peptide Synthesis Core Facility, Department of Pathobiology, Texas A&M University). 1-Hydroxy-7-azabenzotriazole (HOAT) with diisopropylcarbodiimide was used for activation. The yield of pure peptide product was 0.3–0.5 g of peptide/g of the poly(ethylene glycol) resin with PAL-linker. The peptide was cleaved from the solid polymer support, side chain protecting groups were removed by incubation with 90% trifluoroacetic acid/ethanedithiol/thioanisole/anisole (90/3/5/2) for 2 h, and the cleaved peptide was filtered into cold diethyl ether. The resin was then rinsed repeatedly with trifluoroacetic acid followed by cold diethyl ether to completely recover the peptide. The extracted peptide was then dried under N₂ and lyophilized.

Gel filtration chromatography based on molecular weight was used to remove organic contaminants and to partially separate incomplete peptides. Fractions corresponding to absorbance peaks at 215 nm were collected, lyophilized, and further purified by reverse-phase HPLC with a C4 column (Waters) and UV detection at 220 nm.

Plasma desorption mass spectrometry was used to differentiate the full-length peptide product and any byproduct that differs from the target peptide theoretical molecular weight. Plasma desorption mass spectra were obtained for each peptide (Laboratory for Biological Mass Spectrometry, Department of Chemistry, Texas A&M University).

The concentration of peptide stock solution was determined by amino acid analysis (Protein Chemistry Laboratory, Department of Chemistry, Texas A&M University).

Preparation of Small Unilamellar Vesicles (SUV). Small unilamellar vesicles (SUV) composed of phosphatidylcholine, cholesterol (or DHE), and phosphatidylserine (mole ratios of 65:35:0, 35:35:30, or 55:35:10) were prepared by sonication basically as described earlier (45, 46) with some modifications: Lipid CHCl₃ stock solutions were mixed, dried slowly under N₂ to form a thin film on the wall of an acid-washed amber glass vial, and rehydrated in MOPS buffer (10 mM, pH = 7.4, prefiltered through a 0.2 μ m filter) (Millipore, Bedford, MA). The rehydrated sample was then vortexed followed by sonication under N₂ protection in a cold water bath, using a Sonic Dismembrator Model 550 (Fisher Scientific Inc., Pittsburgh, PA). The microprobe energy was maintained at level 4 and programmed for 1 min pauses between 2 min sonication periods to prevent overheating. Multilamellar vesicles and titanium debris from the sonicator probe were removed by centrifugation at 35K rpm for 4 h using a 40Ti rotor (Beckman Instruments, Fullerton, CA) at 4 °C. A lipid phosphate assay was used to determine the lipid concentration of the final SUV solution.

Intermembrane Sterol Exchange Assay. The intermembrane exchange of dehydroergosterol (DHE) for cholesterol

was monitored by a fluorescent assay not requiring separation of donor from acceptor membranes (46–49). The final SUV membrane lipid concentration in the exchange assay was maintained at 150 μ M with 10-fold excess of acceptor over donor vesicles. The vesicle composition was the same for donors and acceptors except for the nature of the sterol (35 mol % DHE in donor vesicles versus 35 mol % cholesterol in acceptor vesicles). During the exchange assay, the sample was continuously stirred at 24 °C in the cuvette with a microstirbar (Fisher Scientific Inc., Pittsburgh, PA). The extent of sterol transfer was monitored by continuous measurement of DHE polarization using a PC1 photon counting fluorometer (ISS Instruments Inc., Champaign, IL) in the T-format. Data were collected automatically, generally every 30 s. The light source was a 300 W xenon arc lamp. The excitation and emission wavelengths were set to 325 and 376 nm, respectively. Potential inner-filter effect and light scattering artifacts were made negligible by using dilute vesicle suspensions (absorbance at 325 nm was <0.1) and by using a KV 389 low-fluorescence cutoff filter in the emission system. Two types of control experiments were performed: (i) Sterol exchange experiments were first carried out with donor membranes in the absence of acceptor membranes, SCP₂, or peptides in order to determine donor stability over the time period and conditions of the experiment. (ii) To ensure that addition of SCP₂ and/or SCP₂ N-terminal peptides to donor membranes in the absence of acceptor membranes did not alter the stability of the DHE polarization signal over time, experiments were performed with donors in the presence of 1.5 μ M SCP₂ and/or 50 μ M SCP₂ N-terminal peptides (^{1–32}SCP₂, ^{10–32}SCP₂, ^{1–24}SCP₂, ^{1–E20–32}SCP₂).

The intermembrane sterol exchange was determined in the presence of both acceptors and donors. Spontaneous intermembrane sterol exchange was performed by measuring the DHE polarization of donor SUV for 10 min to establish a baseline. Thereafter, a 10-fold excess of acceptor SUV was added, and polarization was measured continuously for 3 h. The effects of SCP₂ and/or SCP₂ N-terminal peptides on intermembrane sterol transfer were determined by measuring DHE polarization of donor SUV in the presence of SCP₂ and/or SCP₂ N-terminal peptides for 10 min to establish the baseline. Thereafter, a 10-fold excess of acceptor SUV was added, and polarization was measured continuously for 3 h or until the exchange curve reached a maximal value.

Calculation of the Initial Rate of Molecular Sterol Transfer. While DHE polarization changes can be used to monitor intermembrane sterol transfer, polarization changes do not correlate directly with the molecular (i.e., mass) sterol transferred (46, 49). Therefore, initial rates of DHE polarization change, calculated from the slope of the initial linear portion of the DHE exchange curve, were converted to initial rates of molecular sterol transfer (nanomoles per minute) according to a previously published procedure (46, 49). As described therein, the change in DHE polarization during the exchange best fits the polynomial function:

$$P = -aX_D^2 + bX_D + c \quad (1)$$

where $a = 0.185$, $b = 0.028$, and $c = 0.320$ for the SUV described herein. The equation that links the initial rate of fluorescence polarization change and initial rate of molecular

DHE transfer between SUV was then derived from eq 1. Taking the time derivative for both sides of eq 1 yielded

$$dP/dt = -2aX_D dX_D/dt + b dX_D/dt \quad (2)$$

When $t \rightarrow 0$, $X_D \rightarrow 1$, and rearrangement of eq 2 yielded

$$dX_D/dt|_{t=0} = 1/(b - 2a)(dP/dt)|_{t=0} \quad (3)$$

Considering that the sterol exchange experiments were carried out at 13.6 μ M (total lipid concentration) donor SUV membranes, that donor SUV membranes contained 35% (mol %) of DHE, and that the value of $a = 0.185$ and $b = 0.028$, the initial rate expressed as molecular DHE transfer was obtained:

$$\text{initial rate} = (d[\text{DHE}]/dt)|_{t=0} = -13.9(dP/dt)|_{t=0} \quad (4)$$

The final units for the initial rate is nanomoles per minute.

Resolution of Sterol Domain Kinetics: Fractions and Half-Times. To resolve molecular sterol transfer into multiple kinetic domains, DHE polarization curves obtained from dehydroergosterol exchanges between donor and acceptor SUV were fitted polynomials, and kinetic domain fractions and half-times were resolved as described previously (10, 13, 46, 46, 49). If the sterol exchange is a one-exponential process

$$X_D = f_1 \exp(-kt) + f_2 \quad (5)$$

then polarization P will be a two-exponential function of time. Insertion of eq 5 into eq 1 yielded

$$P = -af_1^2 \exp(-2kt) + (-2af_1f_2 + bf_1) \exp(-kt) - af_2^2 + bf_2 + c \quad (6)$$

where k is the rate constant, f_1 is the fraction of the exchangeable sterol pool, and f_2 is the fraction of the nonexchangeable pool. Constants a , b , and c are from eq 1. Therefore, there are two fitting parameters: k and f_1 . f_2 can be obtained from $f_2 = 1 - f_1$. The final units for half-times are minutes, and the units for fractions are mole fractions.

If the sterol exchange is a two-exponential process, P will be a five-exponential function of time (equation not shown). Under our experimental conditions and SUV lipid contents, the sterol exchanges were best fitted to a one-exponential process. Therefore, eq 6 was used in the curve fittings.

Relationship between Initial Rate and Half-Time of Molecular Sterol Transfer. On the basis of eqs 1–5 above, it is possible to derive an expression which describes the relationship between the initial rate (molar fraction of sterol) of sterol exchange in terms of the half-time of sterol exchange, i.e.

$$\text{initial rate} = -[(dP/dt)|_{t=0}/2(dP/dt)|_{t_{1/2}}]f_1k \exp(-kt_{1/2}) \quad (7)$$

where $(dP/dt)|_{t=0}$ is the initial rate of polarization change, $(dP/dt)|_{t_{1/2}}$ is the rate of polarization change at $t_{1/2}$, and f_1 and k are the preexponential constant and the rate constant, respectively, derived for the kinetic expression for X (see eq 5).

Now, the basic assumptions behind the exchange of sterol between model membranes are considered. First, from the

standard curve, it follows that

$$(dP/dt)|_{t \rightarrow 0} > (dP/dt)|_{t_{1/2}} > 0 \quad (8)$$

That is, there is a distinct difference between the regimes of the initial polarization change and the polarization change at the half-time for any given sterol exchange observing the standard curve. Second, for a set of exchanges in which the half-times vary from any real value to near zero, it is assumed that all the exchanges observe the same standard curve. The limiting polarization at infinite time of exchange must be a constant, as required for the standard curve. Indeed, the Results showed this to be the case.

Now, neglecting the first part of eq 7, which has the polarization changes at the beginning of exchange and at the half-time, there is an exponential expression involving the term $-kt_{1/2}$. This expression yields a curve which has an exponential rise as $t_{1/2}$ varies from 11.6 to 0 (curve not shown). This curve explains a large part of the exponential behavior of $t_{1/2}$ near zero. It will be noted that for values higher than near zero the curve flattens out and may be approximated by a straight line. However, this explanation is by no means the full account of the behavior of the plot of initial rate vs half-time, since the portion of eq 7 involving the polarization changes has been so far neglected. So, taking into account the previously neglected portion of eq 7 and recalling the basic definitions of dP/dt , the following expression may be obtained:

$$[(dP/dt)|_{t \rightarrow 0} / 2(dP/dt)|_{t_{1/2}}] = [(dP/dx)|_{x=1}(dx/dt)|_{t \rightarrow 0}] / [2(dP/dx)|_{x=0.5}(dx/dt)|_{t_{1/2}}] \quad (9)$$

Now, taking the limit as $t_{1/2}$ approaches zero, then $(dx/dt)|_{t_{1/2}}$ approaches $(dx/dt)|_{t \rightarrow 0}$, and $(dP/dx)|_{x=0.5}$ becomes infinitely small, as described in a plot of the mole fraction of sterol, X , vs time (not shown), and hence

$$\lim_{t_{1/2} \rightarrow 0} [(dP/dt)|_{t \rightarrow 0} / 2(dP/dt)|_{t_{1/2}}] = +\infty \quad (10)$$

Thus, in theory, the curve of initial rate vs $t_{1/2}$ should exhibit a rise toward infinity as x is near and approaches zero. However, in reality the standard curve may fail at points very near zero, and so in practice limiting values of initial rate at $t_{1/2}$ near zero will occur. Nevertheless, eq 10 explains the steep upward curvature behavior of eq 7 as $t_{1/2}$ approaches zero.

Determination of SUV Permeability. Membrane permeability was determined by utilizing a fluorescence quenching assay (50–52). In this assay the fluorescence emission of ANTS (i.e., 8-aminonaphthalene-1,3,6-trisulfonic acid disodium salt) is quenched by high concentration of DPX [i.e., *p*-xylenebis(pyridinium bromide)]. By trapping a high concentration of ANTS/DPX within membrane vesicles, the fluorescence of ANTS is effectively quenched by DPX as long as both ANTS and DPX remained trapped inside the vesicle. However, if the vesicle membranes are disrupted (i.e., permeabilized), then ANTS and DPX would leak out of the vesicle and become greatly diluted in the medium, and the fluorescence intensity of ANTS would increase due to release from quenching by DPX. The assay was performed as follows:

First, the SUV containing trapped ANTS/DPX at quenching concentrations were prepared. Stock solutions of POPC, cholesterol, and DOPS in chloroform were measured, mixed, evaporated to dryness under N_2 , and dried in vacuo for at least 4 h. The dried lipids were hydrated with PIPES buffer (20 mM PIPES and 27.5 mM NaCl, pH = 7.4), containing 5 mM ANTS and 50 mM DPX, to yield a 50 mM lipid suspension. The suspension was vortexed for 1 min, bath sonicated for 5 min, and vortexed again for 1 min. To produce SUV containing trapped ANTS/DPX, this suspension was then sonicated under N_2 in a cold water bath, using a Sonic Dismembrator Model 550 (Fisher Scientific Inc., Pittsburgh, PA). The microprobe energy was maintained at level 4 except for 1 min pauses between 2 min sonication periods to prevent overheating. Multilamellar vesicles and titanium debris from the sonicator probe were removed by centrifugation at 35K rpm for 4 h using a 40Ti rotor (Beckman Instruments, Fullerton, CA). The ANTS/DPX-containing SUV were then separated from free dye by size exclusion chromatography using Sephadex G-50. The fractions containing a high concentration of vesicles and no free dye were pooled, and the lipid concentration was determined by the phosphorus assay as described above.

Second, the ANTS/DPX permeability assay was performed by adding an aliquot of the ANTS/DPX-containing SUV to PIPES buffer (20 mM PIPES, 85 mM NaCl, pH = 7.4) \pm SCP₂ and/or SCP₂ N-terminal peptide to obtain a final lipid concentration of 200 μ M in the cuvette. The fluorescence intensity (I_F) of ANTS was then measured as a function of time using a PC1 photon counting fluorescence spectrophotometer (ISS Instruments Inc., Champaign, IL) with the temperature of the sample compartment maintained at 24 °C by a circulating water bath. ANTS was excited at 353 nm, and emission was detected at 525 nm. Excitation and emission monochromator slits were 1.0 and 2.0 nm, respectively. Two neutral density filters, 0.3 and 0.5, were placed in the excitation path to minimize the ANTS photobleaching. A KV389 filter was placed in emission path to minimize the effect of the scattered light while the inner-filter artifact was avoided by maintaining the sample absorbance <0.1 at the wavelength of excitation. Corrections for background fluorescence intensity (I_B) were made by measuring the fluorescence intensity of buffer solutions containing only SUV with trapped ANTS/DPX as well as the fluorescence intensity of buffer solutions containing only the protein/peptides. The total fluorescence intensity (I_T) was determined by measuring the fluorescence intensity after the SUV were completely disrupted by Triton X-100 (0.1%). The percentage of released ANTS was calculated by the equation % release = $100(I_F - I_B)/(I_T - I_B)$. Care was taken to avoid commonly encountered artifacts, such as the inner-filter effect.

Membrane Fluidity Measurements. Membrane fluidity was measured by monitoring the depolarization of the fluorescent probes dehydroergosterol (DHE) and diphenylhexatriene (DPH) in SUV membranes. SUV containing the fluorescent probe DPH were prepared by incubating SUV with DPH at DPH:lipid = 1:250 (molar ratio) for 1 h at 37 °C in the dark. SUV containing the fluorescent probe DHE were made by mixing DHE with the other lipids before SUV were prepared (as described above). The polarization of the probes in SUV, with and without the presence of SCP₂ and/or ¹⁻³²SCP₂, was

measured using an ISS photon counting fluorometer (ISS, Champaign, IL) as described in the SUV–sterol exchange experiments.

Fluorescence Lifetime Determination by Phase and Modulation Fluorometry. Fluorescence lifetimes of DHE (45, 47) and diphenylhexatriene (53–56) were measured by a GREG multifrequency phase and modulation fluorometer (ISS Instruments Inc., Champaign, IL) basically as described in the cited papers. The light source was a He/Cd laser (Model 4240NB; Liconix, Sunnyvale, CA), whose emission intensity at 325 nm was modulated sinusoidally with a Pockels cell. Fluorescence emission was observed through a GC-375 sharp cutoff filter (Janos Technology Inc., Townshend, VT) to eliminate scattered light. Fourteen modulation frequencies were utilized between 10 and 350 MHz. At each frequency, both phase and modulation of the fluorescence were determined with respect to a reference solution of dimethyl-POPOP (Chemalog Chemical Dynamics Corp., South Plainfield, NJ) in absolute ethanol (lifetime = 1.45 ns). The excitation polarizer was set at 0°, and the emission polarizer was set at the magic angle 55° to eliminate Brownian motion as a determinant of apparent lifetime and polarization effects in general. To avoid inner-filter artifacts, sample absorbance at the excitation wavelengths was <0.1. All data were obtained in PIPES buffer at 24 °C.

Phase and modulation data were collected by a computer using an ISS01 interface (ISS Inc., Champaign, IL). The set of phase and modulation data was statistically analyzed by a nonlinear least-squares routine using software obtained from ISS Inc. (Champaign, IL). Data were acquired until the limit of standard error was reached: 0.04° and 0.2°, for phase and modulation, respectively. The data were best fitted to two-exponential terms. In the latter case, each term was characterized by a lifetime (*T*) and a fractional intensity (*F*). The reduced χ^2 (i.e., χ^2) parameter was used as a criterion for the goodness of fit to the applied model.

Binding of Fatty Acids and Phospholipids to SCP₂ and ¹⁻³²SCP₂. Fatty acid and phospholipid binding to SCP₂ and ¹⁻³²SCP₂ was determined using a fluorescence binding assay previously described (57, 58). Briefly, fluorescence emission spectra were taken after fluorescent fatty acid (NBD-stearic acid) or fluorescent phospholipid (DPH-PC) was incubated with SCP₂ or its peptide ¹⁻³²SCP₂ for 2 min. The fluorescence emission spectra were taken in a 1 cm quartz cuvette with a PC1 photon counting spectrofluorometer (ISS Instruments, Champaign, IL). The final concentrations of NBD-stearic acid, DPH-PC, ¹⁻³²SCP₂, and SCP₂ were 0.1 μM in PIPES buffer. All of the spectra were taken at 24 °C with a circulating water bath. The excitation wavelengths used were 466 nm for NBD-stearic acid and 354 nm for DPH-PC. The emission spectra were corrected for buffer and protein or peptide.

Phosphatidylinositol Transfer Assay. Microsomes were isolated from rat liver as described earlier (59). The microsomal protein content was determined by the BCA protein assay (Pierce, Rockford, IL) according to the procedure provided by the manufacturer following extractions with trichloric acid, ethanol, and acetone. Microsomal phosphatidylinositol was labeled with [2-³H]inositol by incubation of microsomes (20 mg of protein) with 10 μCi of [2-³H]inositol as described previously (59). The unlabeled SUV acceptors (POPC:PI = 98:2) were prepared exactly as described above under the section Preparation of Small Unilamellar Vesicles

(SUV). The phosphatidylinositol transfer assays were performed essentially as described previously (59), except the total reaction volume was reduced to 62.5 μL. Briefly, the labeled microsomes pelleted at 100000g at 4 °C for 1 h were resuspended in SET buffer (0.25 M sucrose, 1 mM EDTA, and 10 mM Tris-HCl, pH = 7.4) to obtain a microsomal suspension with the protein concentration 1.25 mg/mL. A 25 μL aliquot of the phosphatidyl[2-³H]inositol-labeled microsomes was then mixed with an equal volume of SUV to obtain a mixture with the ratio of 1.25 mg of microsomal protein to 1 μmol of SUV lipid. After incubation with 1.6 μM SCP₂, and/or 64 μM ¹⁻³²SCP₂, at room temperature for 30 min, 12.5 μL of sodium acetate–sucrose (0.2 M sodium acetate and 0.25 M sucrose) was added, and the resultant solution was vigorously mixed. The aggregated microsomes were then separated from the SUV by centrifugation at 10000g for 30 min at 4 °C. The supernatant containing the SUV was carefully separated from the microsomal pellet and transferred to a scintillation vial. The microsomes were transferred to another scintillation vial after resuspension in 100 μL of SET buffer. Then 5 mL of scintillation fluid (cytosin; ICN Biomedicals, Inc., Irvine, CA) was added to the mixture, and the radioactivity was measured using a 1600 TR Tri-Carb liquid scintillation analyzer (Packard Instrument Co., Downers Grove, IL). The percentage of phosphatidylinositol transfer was calculated by dividing the radioactivity in the SUV (supernatant) by the total radioactivity in SUV (supernatant) plus microsomes (pellet).

RESULTS

Effect of SCP₂ N-Terminal Peptide ¹⁻³²SCP₂ on Intermembrane Sterol Transfer. Earlier studies demonstrated that a peptide, ¹⁻³²SCP₂, comprising the N-terminal amphipathic α-helical region of SCP₂ is a membrane binding domain of SCP₂ and that both this peptide and the complete protein preferentially interacted with highly curved (e.g., SUV) membranes rich in anionic phospholipid and cholesterol (42, 43). To resolve whether membrane binding via the N-terminal ¹⁻³²SCP₂ peptide in itself accounts for SCP₂-mediated intermembrane sterol transfer, the effect of the ¹⁻³²SCP₂ peptide on intermembrane sterol transfer was examined using a fluorescence polarization assay not requiring separation of donor and acceptor membranes. In this assay, donor SUV membranes were composed of POPC: DHE:DOPS at molar ratio of 35:35:30. DHE fluorescence in the donor SUV membranes is self-quenched (46, 49, 60).

Because many membrane-active peptides (e.g., mellitin, cytolysin) disrupt membranes, it was essential to determine the stability of donor SUV fluorescence polarization in response to ¹⁻³²SCP₂ peptide. As expected, due to self-quenching, polarization values of DHE in donor SUV were low (about 0.15) (Figure 1A, ●). Addition of ¹⁻³²SCP₂ peptide (Figure 1A, ○) or SCP₂ (Figure 1A, ▼) elicited only small changes in DHE polarization immediately after addition but did not significantly alter the DHE polarization over the 3 h time period used for exchange experiments. Therefore, neither the ¹⁻³²SCP₂ peptide nor the SCP₂ protein affected the stability of the donor SUV DHE.

The effect of ¹⁻³²SCP₂ peptide on sterol transfer was compared to that of SCP₂ by examining DHE polarization in the presence of both donor SUV and a 10-fold excess of

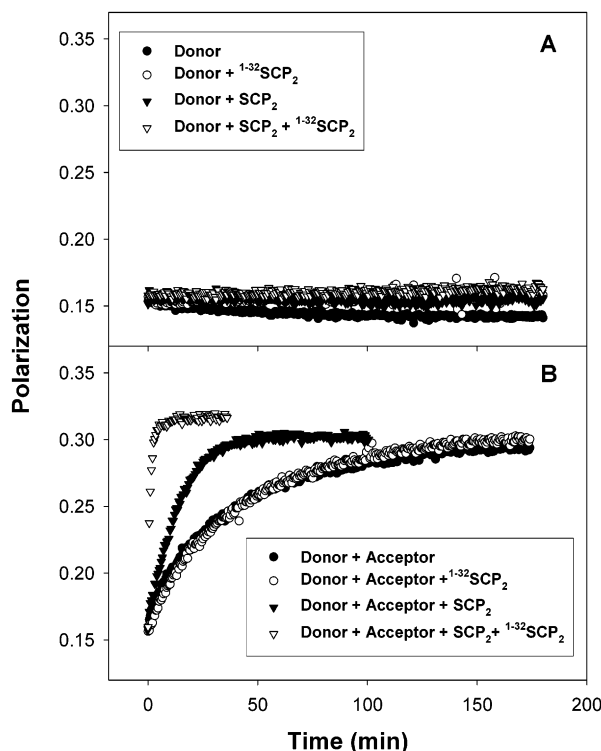


FIGURE 1: Effect of 1^{32}SCP_2 on SCP_2 -mediated sterol transfer between SUV membranes. Donor (POPC:DHE:DOPS = 35:35:30) and acceptor (POPC:cholesterol:DOPS = 35:35:30) SUV membranes were prepared, and sterol exchange assays were performed as described in Experimental Procedures. SCP_2 was $1.5\ \mu\text{M}$, and 1^{32}SCP_2 was $50\ \mu\text{M}$. Panel A: Effect of SCP_2 and/or 1^{32}SCP_2 on fluorescence polarization of DHE in donor SUV membranes (no acceptor SUV) as a function of time: (●) donor SUV only; (○) donor SUV + 1^{32}SCP_2 ; (▼) donor SUV + SCP_2 ; (▽) donor SUV + [SCP_2 + 1^{32}SCP_2]. Panel B: Effect of SCP_2 and/or 1^{32}SCP_2 on fluorescence polarization of DHE in the presence of donor and acceptor SUV membranes: (●) donor SUV + acceptor SUV; (○) donor SUV + acceptor SUV with added 1^{32}SCP_2 ; (▼) donor SUV + acceptor SUV with added SCP_2 ; (▽) donor SUV + acceptor SUV with added [SCP_2 + 1^{32}SCP_2].

acceptor SUV. Acceptor SUV membranes contained cholesterol instead of DHE but at the same molar ratio (POPC:cholesterol:DOPS = 35:35:30). Although the acceptor SUV exhibited no fluorescence, when they were added in 10-fold excess to donor SUV the fluorescence polarization of DHE significantly increased over the 3 h time period of exchange (Figure 1B, ●). This increase was due to the spontaneous transfer of DHE from the donor SUV membrane (wherein DHE was self-quenched leading to low polarization) to the acceptor SUV membrane (wherein DHE concentration was low, resulting in release from self-quenching and increase of polarization). Addition of 1^{32}SCP_2 peptide to the SUV donor/SUV acceptor mixture resulted essentially in the same curve as the spontaneous exchange (Figure 1B, ○), indicating that 1^{32}SCP_2 had no effect on the sterol exchange between SUV membranes. In contrast, addition of SCP_2 greatly enhanced the sterol exchange process (Figure 1B, ▼). Thus the data demonstrated that, in contrast to SCP_2 , the N-terminal peptide 1^{32}SCP_2 did not itself enhance intermembrane sterol transfer.

Potential Synergistic Effects between N-Terminal Peptide 1^{32}SCP_2 and SCP_2 To Elicit Intermembrane Sterol Transfer. To determine if [1^{32}SCP_2 peptide + SCP_2] affected the stability of the donor SUV membranes, [1^{32}SCP_2 peptide

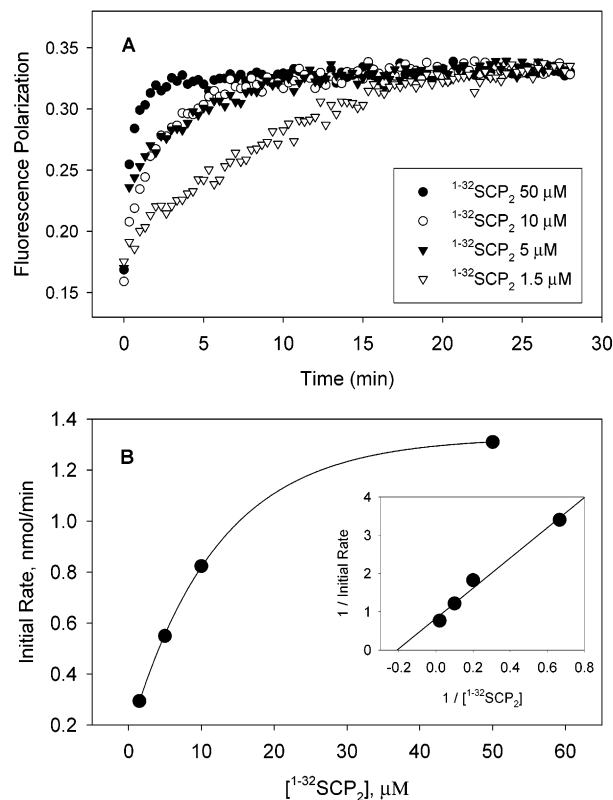


FIGURE 2: Peptide 1^{32}SCP_2 concentration dependence of SCP_2 -mediated sterol exchange. Donor (POPC:DHE:DOPS = 35:35:30) and acceptor (POPC:cholesterol:DOPS = 35:35:30) SUV membranes were prepared, and sterol exchange assays were performed in the presence of $1.5\ \mu\text{M}$ SCP_2 as described in Experimental Procedures. 1^{32}SCP_2 was added over the concentration range of $1.5\text{--}50\ \mu\text{M}$. Panel A: Symbols represent 1^{32}SCP_2 concentration of $1.5\ \mu\text{M}$ (▽), $5\ \mu\text{M}$ (▼), $10\ \mu\text{M}$ (○), and $50\ \mu\text{M}$ (●), respectively. Panel B: The initial rate of SCP_2 -mediated sterol exchange was plotted as function of 1^{32}SCP_2 concentration. Panel B inset shows the double reciprocal plot of $1/\text{initial rate}$ vs $1/[1^{32}\text{SCP}_2]$.

+ SCP_2] was incubated together with donor SUV membranes but in the absence of acceptor SUV membranes (Figure 1A, ▽). The addition of [1^{32}SCP_2 peptide + SCP_2] elicited only small changes in DHE polarization immediately after addition but did not further alter the stability of DHE polarization over the 3 h time period used for exchange experiments. Therefore, [1^{32}SCP_2 peptide + SCP_2] did not synergistically interact to affect the stability of the donor SUV membranes.

The effect of 1^{32}SCP_2 peptide on SCP_2 -mediated sterol transfer was examined in the presence of both donor SUV and a 10-fold excess of acceptor SUV. Addition of [1^{32}SCP_2 + SCP_2] to donor SUV in the presence of acceptor SUV dramatically increased the polarization of DHE over time (Figure 1B, ▽). Even though 1^{32}SCP_2 itself showed no effect on sterol exchange activity of SUV membranes, 1^{32}SCP_2 greatly potentiated the SCP_2 -mediated sterol exchange. This effect of 1^{32}SCP_2 on SCP_2 -mediated sterol exchange increased with increasing concentration of 1^{32}SCP_2 and occurred only at [1^{32}SCP_2] > [SCP_2] (Figure 2A).

N-Terminal Peptide 1^{32}SCP_2 Enhances the Initial Rate of SCP_2 -Mediated Molecular Sterol Transfer. Although the preceding data on DHE polarization changes showed that the N-terminal peptide 1^{32}SCP_2 potentiated the SCP_2 -mediated sterol transfer between membranes, polarization changes do not directly correlate with the molecular (i.e.,

Table 1: Effect(s) of SCP₂, ¹⁻³²SCP₂, and [SCP₂ + ¹⁻³²SCP₂] on Sterol Exchange Kinetics between SUV Model Membranes^a

addition	initial rate (nmol/min)	<i>t</i> _{1/2} (min)	kinetic domain fractions	
			<i>f</i> ₁	<i>f</i> ₂
none	0.052 ± 0.001	43.1 ± 2.5	0.562 ± 0.015	0.438 ± 0.015
¹⁻³² SCP ₂	0.052 ± 0.001	40.0 ± 1.7	0.601 ± 0.015	0.399 ± 0.015
SCP ₂	0.35 ± 0.02 ^b	11.6 ± 0.9 ^b	0.692 ± 0.027 ^b	0.308 ± 0.027 ^b
SCP ₂ + ¹⁻³² SCP ₂	1.00 ± 0.02 ^{b,c}	1.2 ± 0.1 ^{b,c}	0.707 ± 0.020 ^b	0.293 ± 0.020 ^b

^a Sterol exchange assays and data analysis were done as described in Experimental Procedures. Lipid compositions of donor and acceptor SUV were POPC:DHE:DOPS = 35:35:30 and POPC:cholesterol:DOPS = 35:35:30, respectively. SCP₂ was 1.5 μM, and ¹⁻³²SCP₂ was 50 μM. Data represent the mean ± SE, *n* = 5. ^b Refers to *P* < 0.01 as compared to when no protein or peptide was added. ^c Refers to *P* < 0.01 as compared to when only SCP₂ was added.

mass) sterol transferred. Therefore, to obtain a more quantitative view of N-terminal peptide ¹⁻³²SCP₂ effects on molecular transfer of sterol mediated by SCP₂, the initial rates of polarization change were converted to initial rates of molecular sterol transfer according to eq 4 as described in Experimental Procedures.

In the absence of SCP₂ or ¹⁻³²SCP₂, the initial rate of spontaneous molecular sterol transfer between donor SUV and acceptor SUV was 0.052 ± 0.001 nmol/min (Table 1). Addition of ¹⁻³²SCP₂ did not significantly alter the initial rate of molecular sterol transfer (0.052 ± 0.001 nmol/min). In contrast, SCP₂ protein enhanced the initial rate of molecular sterol transfer by 6.7-fold to 0.35 ± 0.02 nmol/min (*P* < 0.01). When both SCP₂ and ¹⁻³²SCP₂ were present together, the initial rate of molecular sterol transfer was increased by 19.2-fold to 1.00 ± 0.02 nmol/min (*P* < 0.01). A plot of the molecular sterol transfer initial rates vs ¹⁻³²SCP₂ concentration was saturable near 50 μM ¹⁻³²SCP₂ (Figure 2B) and, upon transformation of these data to a Lineweaver–Burk plot, yielded a straight line which indicated a *K_m* near 5 μM (Figure 2B, inset).

Clearly, the effects of ¹⁻³²SCP₂ and SCP₂ on the initial rate of molecular sterol transfer were not additive, or antagonistic, but were synergistic. Thus, ¹⁻³²SCP₂ potentiated the ability of SCP₂ to enhance the initial rate of molecular sterol transfer by 2.9-fold, suggesting that ¹⁻³²SCP₂ interacted synergistically with SCP₂ to potentiate the initial rate of SCP₂-mediated molecular sterol transfer.

Effect of N-Terminal Peptide ¹⁻³²SCP₂ on Kinetically Resolved Membrane Sterol Domains. To resolve the half-time and fractional distribution of molecular sterol transfer from the DHE polarization curves during spontaneous sterol transfer between donor and acceptor SUV membranes (Figure 1B, ●), the data were fit to eqs 5–6 (see Experimental Procedures). In the absence of added peptide or protein, spontaneous sterol exchange curves fit very well (*r*² ≥ 0.993) to a one-exponential equation revealing two domains (Table 1): One sterol domain was exchangeable, exhibiting a half-time *t*_{1/2} = 43.1 ± 2.5 min, and accounted for *f*₁ = 0.562 ± 0.015 of total sterol. In contrast, the other sterol domain exhibited a half-time so slow (>3 days) that it could not be accurately measured, even though it accounted for a significant fraction of total sterol; i.e., *f*₂ = 0.438 ± 0.015. Because of the very slow transfer of sterol from the latter domain, it was designated as essentially nonexchangeable.

The N-terminal ¹⁻³²SCP₂ peptide alone did not alter the exchange dynamics of spontaneous molecular sterol transfer. The sterol exchange curve showed that ¹⁻³²SCP₂ alone did not significantly alter the fluorescence polarization of DHE during spontaneous sterol exchange between membranes (Figure 1B, ○). This was confirmed by curve fitting (*r*² ≥ 0.99) that yielded kinetically resolved parameters of molecular sterol transfer which did not significantly differ from those of spontaneous sterol transfer: *t*_{1/2} = 40.0 ± 1.7, *f*₁ = 0.601 ± 0.015, and *f*₂ = 0.399 ± 0.015. While ¹⁻³²SCP₂ appeared to slightly reduce the size of the nonexchangeable fraction *f*₂ from 0.438 ± 0.015 to 0.399 ± 0.015, this effect was not statistically significant. Thus, ¹⁻³²SCP₂ not only did not alter the initial rate of molecular sterol transfer but also did not alter the sterol exchange dynamics of the membranes.

In contrast, addition of SCP₂ altered half-times and fractions of the SUV membrane sterol domains. In the presence of SCP₂ the exchange curve (Figure 1B, ▼) also best fit (*r*² ≥ 0.992) to a one-exponential equation, which yielded one exchangeable domain and one nonexchangeable domain (Table 1). The SCP₂-mediated exchangeable sterol domain exhibited a half-time of *t*_{1/2} = 11.6 ± 0.9 about 3.4-fold faster than that of spontaneous sterol transfer (Table 1). In the presence of SCP₂, the exchangeable domain size (*f*₁ = 0.692 ± 0.027) was increased by 23% over that observed with spontaneous sterol transfer. Concomitantly, the nonexchangeable sterol domain, *f*₂ = 0.308 ± 0.027, was reduced.

To determine if ¹⁻³²SCP₂ potentiated effects of SCP₂ on sterol domains, the sterol exchange assays were carried out with [¹⁻³²SCP₂ + SCP₂]. This sterol exchange curve (Figure 1B, ▽) also best fit (*r*² ≥ 0.98) to a single exponential. In contrast to the lack of effect of ¹⁻³²SCP₂ alone on the kinetically resolved sterol domains in SUV membranes, addition of [¹⁻³²SCP₂ + SCP₂] greatly altered the sterol exchange dynamics (Table 1). Addition of [¹⁻³²SCP₂ + SCP₂] reduced the half-time of sterol transfer by nearly 10-fold to *t*_{1/2} = 1.2 ± 0.1 min (compared with 11.6 ± 0.9 min when only SCP₂ was present). Concomitantly, addition of [¹⁻³²SCP₂ + SCP₂] resulted in fractions of exchangeable (*f*₁ = 0.707 ± 0.020) and nonexchangeable domains (*f*₂ = 0.293 ± 0.020) that were not significantly different from those observed when only SCP₂ was added (Table 1). Thus, ¹⁻³²SCP₂ potentiated the effect of SCP₂ on molecular sterol domain dynamics by decreasing the half-times by an additional nearly 10-fold without further affecting the size of sterol domains.

In summary, in the absence of SCP₂ and ¹⁻³²SCP₂, SUV membranes (POPC:cholesterol:DOPS molar ratio 35:35:30) exhibited two sterol domains, i.e., exchangeable and nonexchangeable domains. The addition of the N-terminal peptide ¹⁻³²SCP₂ alone did not alter either the half-times or size of sterol domains in SUV membranes. In contrast, addition of SCP₂ enhanced molecular sterol transfer by increasing the size of exchangeable sterol domains but decreasing the half-time of the rapidly transferable sterol domain. In contrast, ¹⁻³²SCP₂ potentiated the action of SCP₂ by nearly 10-fold, reducing the half-time of sterol transfer without further alteration of sterol domain size.

Specificity of the Potentiating Effects of ¹⁻³²SCP₂: Mutant N-Terminal Peptides. Previous site-directed mutagenesis studies of SCP₂ showed that substitutions or deletions in the N-terminal region SCP₂ disrupted the ability to enhance sterol

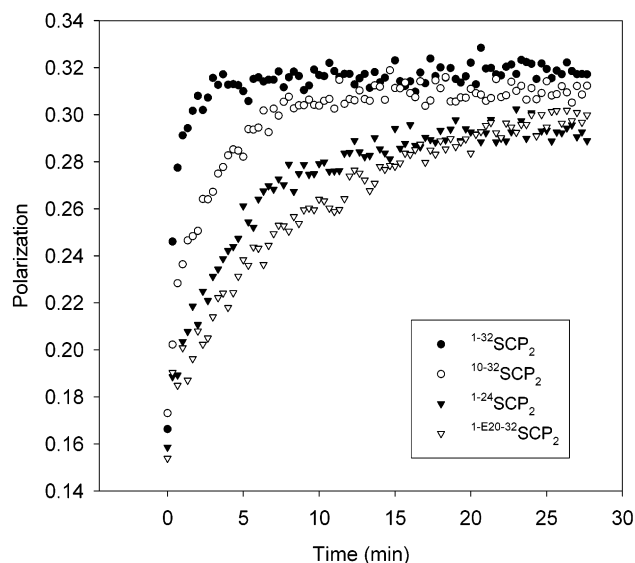


FIGURE 3: Effect of SCP₂ N-terminal peptide structure on SCP₂-mediated sterol transfer between SUV membranes. Donor (POPC:DHE:DOPS = 35:35:30) and acceptor (POPC:cholesterol:DOPS = 35:35:30) SUV membranes were prepared, and sterol exchanges were performed as described in Experimental Procedures. All exchanges were performed in the presence of 1.5 μ M SCP₂ and 50 μ M each of the following SCP₂ N-terminal peptides: ¹⁻³²SCP₂ (●), ¹⁰⁻³²SCP₂ (○), ¹⁻²⁴SCP₂ (▼), and ^{1-E20-32}SCP₂ (▽).

Table 2: Mutations in the SCP₂ N-Terminal Peptide Structure Differentially Alter SCP₂-Mediated Intermembrane Sterol Exchange Kinetics between SUV Model Membranes^a

peptides	initial rate (nmol/min)	<i>t</i> _{1/2} (min)	kinetic domain fractions	
			<i>f</i> ₁	<i>f</i> ₂
¹⁻³² SCP ₂	1.00	1.2	0.71	0.29
¹⁰⁻³² SCP ₂	0.90	2.1	0.67	0.33
¹⁻²⁴ SCP ₂	0.56	3.8	0.54	0.46
^{1-E20-32} SCP ₂	0.32	7.4	0.61	0.39

^a Sterol exchange assays and data analysis were done as described in Experimental Procedures. Lipid compositions of donor and acceptor SUV were POPC:DHE:DOPS = 35:35:30 and POPC:cholesterol:DOPS = 35:35:30, respectively. SCP₂ was 1.5 μ M, and the peptides were 50 μ M. Data presented are single measurements.

transfer (31). Subsequently, it was shown that SCP₂ N-terminal peptides mimicking the same modifications disrupted the ability of these peptides to bind to membranes in the order ¹⁻³²SCP₂ > ¹⁰⁻³²SCP₂ > ¹⁻²⁴SCP₂ > ^{1-E20-32}SCP₂ (42, 43). Therefore, the effects of these modified peptides on SCP₂-mediated sterol exchange were tested to see if their membrane binding ability correlated with their effects on SCP₂-mediated sterol exchange.

Similar to ¹⁻³²SCP₂, none of the peptides by themselves affected the DHE polarization during intermembrane sterol exchange (data not shown). However, in the presence of SCP₂, the peptides differed in their abilities to potentiate the ability of SCP₂ to increase sterol exchange: ¹⁻³²SCP₂ (Figure 3, ●) > ¹⁰⁻³²SCP₂ (Figure 3, ○) > ¹⁻²⁴SCP₂ (Figure 3, ▼) > ^{1-E20-32}SCP₂ (Figure 3, ▽). The initial rates, half-times, and kinetic domain fractions of molecular sterol transfer calculated from the polarization in Figure 3 are presented in Table 2. When both peptide and SCP₂ were present, the initial rates of molecular sterol transfer were 1.00, 0.90, 0.56, and 0.32 nmol/min for ¹⁻³²SCP₂, ¹⁰⁻³²SCP₂, ¹⁻²⁴SCP₂, and ^{1-E20-32}SCP₂, respectively. Likewise, when both peptide and

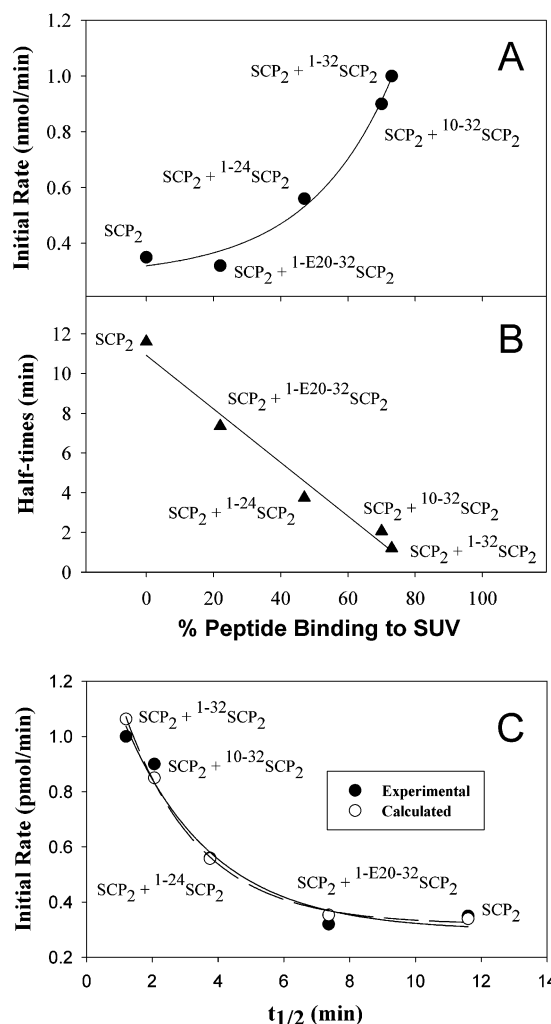


FIGURE 4: Correlation between percent peptide binding to SUV and effect of the peptide on SCP₂-mediated sterol transfer kinetics. The sterol exchange assays and data analysis were performed as described in Experimental Procedures. The SCP₂ concentration was kept at 1.5 μ M, and peptide concentrations were 50 μ M. Data for peptide binding to SUV membranes (POPC:cholesterol:DOPS = 35:35:30) were taken from ref 42. Values represented single measurements. Panel A: Plot of initial rate of molecular sterol transfer vs percent peptide binding to SUV. Panel B: Plot of half-time of molecular sterol transfer vs percent peptide binding. Panel C: Plot of initial rate of molecular sterol transfer vs half-time of molecular sterol transfer. In panel C the solid line refers to experimental data points while the dashed line refers to calculated values from eq 7.

SCP₂ were present, the half-times of molecular sterol transfer were 1.2, 2.1, 3.8, and 7.4 min for ¹⁻³²SCP₂, ¹⁰⁻³²SCP₂, ¹⁻²⁴SCP₂, and ^{1-E20-32}SCP₂, respectively.

These effects of the respective peptides on SCP₂-mediated molecular sterol transfer parameters were in exactly the same order as the membrane binding ability of the respective peptides (42, 43). Using the percent peptide binding to SUV obtained earlier (42), it was possible to plot the initial rate and half-time of molecular sterol transfer with increasing peptide binding. As the percent peptide bound to SUV increased, the initial rate of SCP₂-mediated molecular sterol transfer increased exponentially (Figure 4A). In contrast, with increasing percent peptide binding to SUV the half-time of molecular sterol transfer decreased linearly (Figure 4B). The fact that both curves are not linear is not an apparent

Table 3: Influence of SCP₂ and N-Terminal Peptides on Membrane Permeability: SUV Leakage Assay^a

protein or peptide	protein or peptide concn (μM)	% release, mean ± SE (n)
melittin	2.5	64 ± 3 (3)
	5.0	100
SCP ₂	1.5	-1.6 ± 0.3 (3)
	3	1.3 (1)
	4	-2.9 (1)
1-32SCP ₂	100	-0.7 ± 0.6 (3)
1-24SCP ₂	100	-0.7 ± 1.1 (2)
1-E20-32SCP ₂	100	-0.6 ± 1.2 (2)
10-32SCP ₂	100	-0.6 ± 1.0 (2)

^a The ANTS leakage assay from SUV was done as described in Experimental Procedures. The percentage of released ANTS was calculated by the equation % release = 100($I_F - I_B$)/($I_T - I_B$), where I_F is the measured fluorescence intensity, I_B is background fluorescence intensity, and I_T is the total fluorescence intensity.

discrepancy in the data. Instead, it is based on the nonlinear relationship between initial rate and half-time of molecular sterol transfer (Figure 4C, solid circles, solid line). These experimental data were closely fit by calculated values based on eq 7 (Figure 4C, open circles, dashed line) derived as described in Experimental Procedures. As shown in Experimental Procedures, for a given set of $t_{1/2}$ approaching zero which follow one identical standard curve, it was predicted that the initial rates should rise sharply as $t_{1/2}$ approaches zero. This occurred because of the conditions stated in eq 8; i.e., as $t_{1/2}$ approaches zero, $(dP/dt)|_{t \rightarrow 0}$ tries to approach $(dP/dt)|_{t \rightarrow 0}$. However, as stated in eq 8, $(dP/dt)|_{t \rightarrow 0}$ can never approach $(dP/dt)|_{t \rightarrow 0}$, and so the values of $(dP/dt)|_{t \rightarrow 0}$ are pushed even higher, in asymptotic behavior. A plot of experimental and calculated values of initial rate and half-time confirmed the validity of eq 7, as the calculated value of initial rate approximated the experimental data (Figure 4C). Each curve has an r^2 of at least 0.96. It must be noted that eq 7 is an approximation, as other terms which are close to zero have been omitted and therefore did not contribute significantly to the final result. Consequently, this derivation leads to only a slight error in the curvature of the calculated curve as compared to the experimental curve.

Effect of SCP₂ and N-Terminal Peptides on Membrane Structure: Permeability Assay. Since some membrane-active peptides (e.g., mellitin, cytolysin) disrupt membrane structure and significantly alter membrane permeability (50–52), it was important to determine if the action of SCP₂ N-terminal peptides and/or SCP₂ on enhancing intermembrane sterol transfer was the result of membrane disruption. To test this possibility, a membrane permeability assay was performed. Briefly, SUV were prepared containing the trapped fluorophore/quencher ANTS/DPX as described in Experimental Procedures. Leakage of ANTS/DPX from the SUV was tested in the presence of mellitin as a positive control (Table 3). At 2.5 and 5 μM mellitin, the SUV were disrupted such that 64% and 100%, respectively, of the entrapped dye was released (Table 3). However, when the same leakage experiments were performed with SCP₂, no significant leakage was observed with SCP₂ at concentrations as high as 4 μM (3-fold higher than used in intermembrane sterol exchange assays). Likewise, no significant leakage was observed with any of the peptides at concentrations as high as 100 μM (Table 3). These results showed that neither SCP₂ nor any of its N-terminal peptides disrupted membrane

Table 4: Effect of SCP₂ and N-Terminal Peptides on SUV Membrane Fluidity As Determined by Diphenylhexatriene Polarization^a

protein or peptide	polarization		
	no addition	protein and/or peptide	ΔP
Anionic SUV (35:35:10)			
SCP ₂	0.2563 ± 0.0029	0.2672 ± 0.0018 ^b	0.011 ± 0.003
1-32SCP ₂	0.2423 ± 0.0015	0.2486 ± 0.0005 ^c	0.006 ± 0.002
[SCP ₂ + 1-32SCP ₂]	0.2475 ± 0.0014	0.2781 ± 0.0026 ^c	0.031 ± 0.003
polylysine	0.2769 ± 0.0016	0.3277 ± 0.0033 ^c	0.051 ± 0.004
Neutral SUV (65:35)			
SCP ₂	0.2991 ± 0.0008	0.2982 ± 0.0008	0.001 ± 0.001
1-32SCP ₂	0.2991 ± 0.0008	0.2993 ± 0.0008	0.000 ± 0.001
[SCP ₂ + 1-32SCP ₂]	0.2991 ± 0.0008	0.2994 ± 0.0007	0.000 ± 0.001
polylysine	0.2991 ± 0.0008	0.2996 ± 0.0004	0.001 ± 0.001

^a SUV (POPC:cholesterol = 65:35) or SUV (POPC:cholesterol:DOPS = 35:35:30) were prepared as described in Experimental Procedures. SUV were incubated with diphenylhexatriene (DPH) at DPH:lipid = 1:250 (molar ratio) at 37 °C in the dark for 1 h. Polarization was measured 2 min after addition of SCP₂ (1.5 μM) and/or peptide (50 μM) as described in Experimental Procedures. ^b Refers to $P < 0.05$ as compared to no added proteins and/or peptides. ^c Refers to $P < 0.01$ as compared to no added proteins and/or peptides.

structure to increase membrane permeability to trapped water-soluble molecules. Therefore, the ability of SCP₂ to enhance membrane sterol exchange and SCP₂ N-terminal peptides' ability to potentiate SCP₂-mediated sterol exchange were not due to membrane disruption.

Effect of SCP₂ and N-Terminal Peptides on Membrane Structure: Membrane Fluidity Determined with Diphenylhexatriene. Membrane fluidity was measured by monitoring the polarization of the fluorescent probe diphenylhexatriene (DPH) at nonquenching low mole percent in the SUV membrane. DPH is a hydrophobic molecule that distributes uniformly in both "fluid" and "solid" regions of the membrane and thus monitors the "average" hydrophobic membrane environment (55). If SCP₂ or its N-terminal peptide 1-32SCP₂ bound to membranes to alter the fluidity of the membrane, then the DPH fluorescence polarization should decrease. Addition of SCP₂ or 1-32SCP₂ did not decrease DPH polarization in the anionic SUV (POPC:cholesterol:DOPS = 35:35:30) membranes (Table 4). On the contrary, the DPH polarization was increased ($P < 0.01$) in both cases. Addition of [SCP₂ + 1-32SCP₂] also increased DPH polarization in the anionic SUV (POPC:cholesterol:DOPS = 35:35:30) membranes, and the effect was not simply additive (Table 4). Instead, the DPH polarization increase upon adding [SCP₂ + 1-32SCP₂] was synergistic, being 2-fold greater than the sum of either alone (Table 4). These effects were specific for anionic phospholipid-containing SUV membranes and did not occur with neutral charged SUV membranes (Table 4). Likewise, SCP₂ and/or 1-32SCP₂ bind(s) to anionic phospholipid-containing SUV but not neutral SUV (POPC:cholesterol = 65:35) (42).

Together, these data show that neither SCP₂ and/or 1-32SCP₂ interaction with the anionic SUV membranes fluidized the membrane. A slight increase in polarization showed that SCP₂ and/or 1-32SCP₂ binding to the membrane increased the rigidity of the membrane. The rigidifying effect of SCP₂ and/or 1-32SCP₂ was similar to that observed with

Table 5: SCP₂ and ¹⁻³²SCP Effects on Diphenylhexatriene Fluorescence Intensity^a

protein or peptide added	relative fluorescence intensity		
	no addition	SCP ₂ and/or ¹⁻³² SCP ₂	intensity increase
+DPH			
SCP ₂	1.5 ± 0.1	3.1 ± 0.6 ^b	1.6 ± 0.6
¹⁻³² SCP ₂	0.4 ± 0.3	1.9 ± 0.5 ^b	1.5 ± 0.6
[SCP ₂ + ¹⁻³² SCP ₂]	0.2 ± 0.4	2.0 ± 0.4 ^b	1.8 ± 0.6
+[SUV with DPH]			
SCP ₂	101 ± 7	133 ± 8 ^b	32 ± 11
¹⁻³² SCP ₂	119 ± 4	128 ± 4	9 ± 6
[SCP ₂ + ¹⁻³² SCP ₂]	81 ± 6	119 ± 3 ^c	38 ± 7

^a SUV (POPC:cholesterol:DOPS = 35:35:30) were prepared and incubated with diphenylhexatriene (DPH) at DPH:lipid = 1:250 (molar ratio) at 37 °C in the dark for 1 h as described in Experimental Procedures. The fluorescence intensity was measured before (i.e., no addition) and after SCP₂, ¹⁻³²SCP₂, or [SCP₂ + ¹⁻³²SCP₂] was added. Background fluorescence intensity (i.e., SCP₂ only in buffer, ¹⁻³²SCP₂ only in buffer, or [SCP₂ + ¹⁻³²SCP₂] only in buffer) in the absence of DPH was subtracted from the corresponding measurement data. Values represent the mean ± SE, *n* = 4. ^b Refers to *P* < 0.05 as compared to no added proteins and/or peptides. ^c Refers to *P* < 0.01 as compared to no added proteins and/or peptides.

polylysine, a synthetic peptide with multiple positive charges, that is known to bind to the negative membranes (Table 4). SCP₂, ¹⁻³²SCP₂, and polylysine are both cationic polypeptides. It should be noted that the increase in DPH polarization upon membrane binding of the SCP₂ or ¹⁻³²SCP₂ peptide was specific for anionic phospholipid-containing SUV.

The increase in DPH polarization upon membrane binding of the SCP₂ or ¹⁻³²SCP₂ peptide was not due to direct extraction/interaction of these polypeptides with DPH. Diphenylhexatriene, a nonpolar molecule, fluoresced weakly in aqueous buffer as opposed to membranes as shown by relative fluorescence intensities in buffer and SUV of 1.5 and 101.3, respectively. Addition of diphenylhexatriene to SCP₂, ¹⁻³²SCP₂, or [SCP₂ + ¹⁻³²SCP₂] in buffer increased the fluorescence intensity slightly by 1.6, 1.4, and 1.8 fluorescence units, respectively (Table 5). These increases, although statistically significant, were barely above the background value as compared to diphenylhexatriene in SUV membranes. Furthermore, addition of SCP₂, ¹⁻³²SCP₂, or [SCP₂ + ¹⁻³²SCP₂] to diphenylhexatriene in SUV increased the fluorescence intensity by 30, 9, and 36, respectively (Table 5). These 6–20 larger increases in diphenylhexatriene intensity in the SUV were consistent with the increased polarization values (Table 4) indicating increased rigidity of the membrane upon addition of SCP₂, ¹⁻³²SCP₂, or [SCP₂ + ¹⁻³²SCP₂].

Effect of SCP₂ and N-Terminal Peptides on Membrane Structure: Binding of Membrane Sterol. As indicated in the Experimental Procedures, in SUV comprised of POPC:DHE:DOPS (35:35:30) the DHE is self-quenched and exhibits low polarization. In contrast, DHE bound to SCP₂ has a significantly higher polarization (29, 30). Thus, if SCP₂ or its N-terminal peptide ¹⁻³²SCP₂ bound and/or extracted DHE from the SUV, then the DHE fluorescence polarization should increase. Two types of experiments were performed to determine if SCP₂ and/or ¹⁻³²SCP₂ peptide bound sterol.

At time *t* = 0 in the fluorescent sterol exchange assay, the DHE is maximally self-quenched and polarization exhibits the lowest value of 0.1522 ± 0.0005 (Table 6, *t* =

Table 6: Effect of SCP₂ and ¹⁻³²SCP₂ on DHE Fluorescence Polarization in SUV^a

addition	polarization	
	<i>t</i> = 0	<i>t</i> = ∞
none	0.1522 ± 0.0005	0.294 ± 0.004
SCP ₂	0.1588 ± 0.0009 ^b	0.309 ± 0.003 ^b
¹⁻³² SCP ₂	0.1530 ± 0.0011	0.300 ± 0.004
SCP ₂ + ¹⁻³² SCP ₂	0.1609 ± 0.0022 ^c	0.312 ± 0.003 ^c

^a SUV lipid compositions of donor and acceptor are POPC:DHE:DOPS = 35:35:30 POPC:cholesterol:DOPS = 35:35:30 (molar ratio). The experiments were carried out with total lipid at 25 μM, SCP₂ at 0.25 μM, and ¹⁻³²SCP₂ at 8.3 μM. Polarization was determined at *t* = 0 (i.e., beginning of the exchange assay) and *t* = ∞ (i.e., determined from extrapolation of the polarization curve to infinity). Polarization values represent the mean ± SE, *n* = 4–5. ^b Refers to *P* < 0.05 as compared to no addition. ^c Refers to *P* < 0.01 as compared to no addition.

Table 7: Effect(s) of SCP₂ and ¹⁻³²SCP₂ on DHE Fluorescence Lifetime in SUV^a

addition	τ ₁ (ns)	<i>f</i> ₁	τ ₂ (ns)	<i>f</i> ₂
none	0.84 ± 0.01	0.87 ± 0.01	2.68 ± 0.17	0.13 ± 0.01
SCP ₂	0.97 ± 0.03 ^c	0.94 ± 0.01 ^c	4.92 ± 0.60 ^c	0.06 ± 0.01 ^c
¹⁻³² SCP ₂	0.93 ± 0.01 ^c	0.88 ± 0.01	3.87 ± 0.16 ^b	0.12 ± 0.01

^a SUV [300 μM, lipid composition POPC:DHE:DOPS = 35:35:30 (molar ratio)] were prepared as described in Experimental Procedures. SCP₂ was 4 μM, and ¹⁻³²SCP₂ was 15 μM. Lifetime components τ₁ and τ₂ as well as their respective fractions (*f*₁ and *f*₂) were determined as indicated in Experimental Procedures. Values represent the mean ± SE, *n* = 4–7. ^b Refers to *P* < 0.05 as compared to SUV only (none). ^c Refers to *P* < 0.01 as compared to SUV only (none).

0). When SCP₂ was added to the SUV containing DHE, polarization increased significantly (*P* < 0.05) from 0.1522 ± 0.0005 to 0.1588 ± 0.0009, an increase of 0.0066 polarization unit (Table 6, *t* = 0). In contrast, when the N-terminal peptide ¹⁻³²SCP₂ was added, there was no significant change in DHE polarization. Binding of [SCP₂ + ¹⁻³²SCP₂] elicited the same polarization change as SCP₂ alone.

At time *t* = ∞ in the DHE exchange assay, the DHE is released from self-quenching and exhibits a 2-fold higher polarization of 0.294 ± 0.004 (Table 7, *t* = ∞). Upon addition of SCP₂ the polarization of DHE increased significantly (*P* < 0.05) from 0.294 ± 0.0045 to 0.309 ± 0.003, an increase of 0.015 polarization unit (Table 6, *t* = ∞). Again, when the N-terminal peptide ¹⁻³²SCP₂ was added, there was no significant change in DHE polarization. Binding of [SCP₂ + ¹⁻³²SCP₂] elicited the same polarization change as SCP₂ alone. Interestingly, the SCP₂-induced increase in DHE polarization in SUV at *t* = ∞ (no DHE self-quenching) was > 2-fold greater than at *t* = 0 (maximal DHE self-quenching). Since SCP₂ shifted a greater proportion of DHE into the exchangeable pool at *t* = ∞ (Table 1), this suggested that SCP₂ bound DHE preferentially from the exchangeable DHE pool.

Thus, these data indicate that SCP₂, but not ¹⁻³²SCP₂ peptide, bound DHE in the SUV membrane. Likewise, the ¹⁻³²SCP₂ peptide did not synergistically enhance the DHE binding to SCP₂. However, the amount bound represented only a small fraction of the total sterol in the membrane.

SCP₂ and ¹⁻³²SCP₂ Effects on the Fluorescence Lifetime of DHE in Membranes. Phase and modulation fluorometry

showed that DHE in SUV (POPC:DHE:DOPS molar ratio 35:35:30) exhibited two lifetimes in the absence of added protein or peptides (Table 7). About 87% of the DHE intensity was due to a short lifetime component, $\tau_1 = 0.84 \pm 0.01$ (ns), while $\sim 13\%$ of the DHE intensity had a longer lifetime, $\tau_2 = 2.68 \pm 0.17$ (ns). In the presence of SCP₂, the fraction of the shorter lifetime of DHE increased from $87 \pm 1\%$ to $94 \pm 1\%$ ($P < 0.01$), and the τ_1 increased from 0.84 ± 0.01 to 0.97 ± 0.03 ns ($P < 0.01$). In contrast, addition of SCP₂ decreased the fraction of the longer lifetime 2-fold from $13 \pm 1\%$ to $6 \pm 1\%$ ($P < 0.01$) and increased τ_2 by 1.8-fold from 2.68 ± 0.17 to 4.92 ± 0.60 ns ($P < 0.01$). Thus, SCP₂ increased the average lifetime of DHE in SUV from 1.08 to 1.21 ns ($P < 0.01$). This was consistent with the known effect of SCP₂ on increasing the lifetime upon binding micellar DHE in aqueous buffer (29). These observations, taken together with the increased polarization of DHE upon addition of SCP₂ to membranes (Table 5), suggest that SCP₂ bound a portion of the DHE in the SUV.

Despite its inability to bind DHE, as evidenced by lack of effect on DHE polarization, addition of ¹⁻³²SCP₂ to SUV membranes significantly altered the DHE lifetime parameters (Table 7). In the presence of ¹⁻³²SCP₂, the fraction of the shorter lifetime of DHE, 88%, was not altered, but the τ_1 increased from 0.84 ± 0.01 to 0.93 ± 0.01 ns ($P < 0.01$). Likewise, addition of ¹⁻³²SCP₂ did not alter the fraction of the longer lifetime component but increased τ_2 by 1.4-fold from 2.68 ± 0.17 to 3.87 ± 0.16 ns ($P < 0.05$). Thus, ¹⁻³²SCP₂ increased the average lifetime of DHE in SUV from 1.08 to 1.29 ns ($P < 0.05$) (Table 7) without altering DHE polarization (Table 6). The lifetime of DHE in the SUV membrane increases with increasing aqueous accessibility (47). Therefore, the effect of ¹⁻³²SCP₂ peptide to increase the DHE lifetime in SUV suggests that ¹⁻³²SCP₂ peptide altered the microenvironment of the DHE in the SUV to become slightly more hydrophilic.

Interaction of ¹⁻³²SCP₂ with Fatty Acids and Phospholipids. Although it is well documented that SCP₂ binds fatty acids and phospholipids (reviewed in refs 1 and 38), it is unknown if its N-terminal peptide ¹⁻³²SCP₂ binds fatty acids or phospholipids. A direct fluorescence binding assay was used to address these questions.

First, NBD-stearic acid, an NBD-labeled 18-carbon saturated fatty acid, was used in the fluorescence binding assay to determine if ¹⁻³²SCP₂ peptide bound to fatty acid. NBD-stearic acid is almost nonfluorescent in aqueous buffer. However, upon binding to proteins such as SCP₂ (57), NBD-stearic acid is now located in a more hydrophobic environment within the ligand binding site of SCP₂, and its fluorescence intensity increases concomitant with an emission maximum shift to lower wavelength. When NBD-stearic acid (0.1 μ M) was incubated with SCP₂ (0.1 μ M), the fluorescence intensity of the NBD-stearic acid increased and its fluorescence emission maximum decreased from 556 to 530 nm (Figure 5A). When the same binding experiment was done with ¹⁻³²SCP₂ (0.1 μ M), the NBD-stearic acid fluorescence emission spectrum was identical with that of NBD-stearic acid in buffer (Figure 5A). This suggested that, unlike SCP₂, the N-terminal peptide ¹⁻³²SCP₂ did not bind NBD-stearic acid.

Second, the fluorescence binding assay was used to investigate if ¹⁻³²SCP₂ binds phospholipids. DPH-labeled

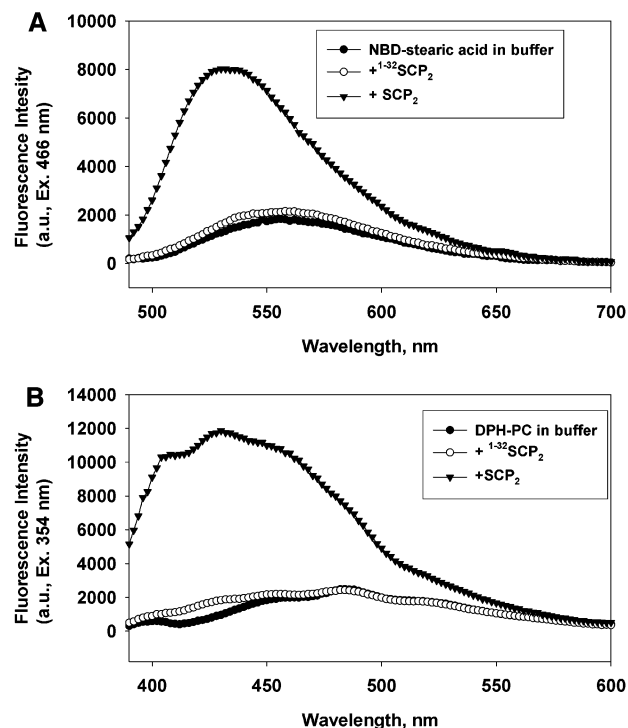


FIGURE 5: SCP₂ and ¹⁻³²SCP₂ binding to fatty acid and phospholipid. A fluorescence binding assay described in Experimental Procedures was used to determine the interaction of NBD-stearic acid and DPH-PC with ¹⁻³²SCP₂ and SCP₂. Concentrations of protein/peptide and ligands were 0.1 μ M. All of the experiments were carried out at 24 °C. Panel A: Fluorescence emission spectra of NBD-stearic acid in buffer (●), and in the presence of ¹⁻³²SCP₂ (○) and SCP₂ (▼). The excitation wavelength was 468 nm. Panel B: Fluorescence emission spectra of DPH-PC in buffer (●) and in the presence of ¹⁻³²SCP₂ (○) and SCP₂ (▼). The excitation wavelength was 354 nm.

phosphatidylcholine (DPH-PC) is almost nonfluorescent in aqueous buffer (Figure 5B). When DPH-PC (0.1 μ M) was incubated with SCP₂ (0.1 μ M), the fluorescence intensity of the DPH-PC increased greatly. When the same binding experiment was done with ¹⁻³²SCP₂ (0.1 μ M), the DPH-PC fluorescence emission spectrum was identical with that in buffer (Figure 5B). This suggested that, unlike SCP₂, its N-terminal peptide ¹⁻³²SCP₂ did not bind DPH-PC.

Effect of ¹⁻³²SCP₂ on Spontaneous and SCP₂-Mediated Phospholipid Transport. As described above, SCP₂ enhanced cholesterol transfer between SUV membranes, a process potentiated by the ¹⁻³²SCP₂ peptide. Although SCP₂ also enhances phospholipid transfer between membranes (reviewed in refs 1 and 38), it is not known whether the ¹⁻³²SCP₂ peptide specifically potentiates only SCP₂-mediated cholesterol transfer or also SCP₂-mediated phospholipid transfer. This question was resolved using a radioactive phosphatidylinositol transfer assay. In the absence of SCP₂ and ¹⁻³²SCP₂, the spontaneous PI transport was about 2.1% (Table 8). When SCP₂ was present, the percent PI transfer increased to 31.1%. When ¹⁻³²SCP₂ was present by itself, the percent PI transfer (2.2%) did not change significantly compared to when no protein or peptide was present. In the presence of both SCP₂ and ¹⁻³²SCP₂ the PI transfer was 35.0%, not significantly different from when only SCP₂ was present. Therefore while SCP₂ was able to increase the PI transfer from 2.1% to 31.1%, its N-terminal peptide did not

Table 8: Effect of SCP₂ and ¹⁻³²SCP₂ on PI Transfer between Membranes^a

buffer	SCP ₂	¹⁻³² SCP ₂	% PI transfer
+	—	—	2.1 ± 0.3
+	+	—	31.1 ± 0.5
+	—	+	2.2 ± 0.4
+	+	+	35.0 ± 2.6

^a PI transfer was measured as described in Experimental Procedures. Values represent the mean percent PI transfer ± SD, *n* = 4. SCP₂ concentration was 1.6 μM, and ¹⁻³²SCP₂ concentration was 64 μM.

directly affect PI transfer or potentiate SCP₂-mediated PI transfer.

DISCUSSION

Previous studies demonstrated that sterol carrier protein-2 (SCP₂) enhances intermembrane sterol transfer not only in vitro (2–12, 12, 13) but also in intact cells (1, 12, 14, 14–18) and animals (19–21, 61, 62). Despite these findings, molecular details of the mechanism(s) whereby SCP₂ mediates intermembrane sterol transfer are only beginning to be resolved. While both membrane binding and ligand binding appear to be essential for SCP₂-mediated cholesterol transfer (41–43), the structural interrelationship between these functions is not yet clear.

The membrane binding domain of SCP₂ appears to reside in the N-terminal α-helix region comprised of amino acid residues 1–32. Studies with SCP₂ and a synthetic peptide comprising the N-terminal 32 amino acids, i.e., ¹⁻³²SCP₂, were consistent with this being the membrane binding domain of SCP₂ (42, 43). Just like SCP₂, ¹⁻³²SCP₂ preferentially binds to anionic (negatively charged) phospholipid-rich, cholesterol-rich, highly curved membranes. Site-directed mutagenesis shows that removal of the N-terminal 1–32 amino acids results in complete loss of SCP₂ function in intermembrane ligand transfer (31). However, it is not known if the membrane binding domain itself is sufficient to mediate sterol exchange activities of SCP₂. In the present investigation, a fluorescent sterol (i.e., DHE) exchange assay not requiring separation of donor and acceptor membranes was used to examine this possibility.

First, it was shown that although SCP₂ mediates sterol transfer from anionic phospholipid-containing membranes (2, 5–7, 60, 63, 64), neither ¹⁻³²SCP₂ nor several modified SCP₂ N-terminal peptides with weaker membrane interaction ability (i.e., ¹⁰⁻³²SCP₂, ¹⁻²⁴SCP₂, ^{1-E20-32}SCP₂) accelerated sterol exchange from anionic phospholipid-containing membranes. Likewise, ¹⁻³²SCP₂ peptide did not enhance intermembrane phosphatidylinositol exchange. Therefore, even though the N-terminal amphipathic α-helix (i.e., ¹⁻³²SCP₂) is critical for SCP₂ binding to anionic phospholipid-containing membranes, this membrane binding domain itself did not directly mediate intermembrane sterol or phospholipid transfer.

Second, although SCP₂ binds sterols (36), the N-terminal membrane binding domain of SCP₂ does not in itself bind sterol, fatty acid, or phospholipid. DHE polarization studies shown herein demonstrated that ¹⁻³²SCP₂ did not bind DHE in anionic phospholipid-rich membranes to increase DHE polarization. In contrast, SCP₂ bound DHE in anionic phospholipid-rich, but not neutral charged, membranes to

increase DHE polarization. The latter finding was supported by earlier data also suggesting that SCP₂ does not bind DHE in neutral membrane vesicles (65). These results demonstrating that SCP₂ binds sterols from membranes are supported by aqueous ligand binding assays which show that SCP₂ binds radiolabeled cholesterol (30) as well as fluorescent sterols such as DHE (29, 30) and NBD-cholesterol (1, 24, 27, 36). Finally, in addition to binding sterols, SCP₂ is known to bind fatty acids and phospholipids (reviewed in refs 1 and 38). While these findings are consistent with the ¹⁻³²SCP₂ peptide not binding sterol, fatty acid, or phospholipid, nevertheless it must be considered that this part of the polypeptide chain (i.e., amino acids 1–32) may still be important for overall folding of SCP₂ and thereby the function of the ligand binding site.

Third, for the first time it was shown that ¹⁻³²SCP₂ potentiated the ability of SCP₂ to elicit intermembrane sterol transfer. This potentiation was specific for sterol transfer since ¹⁻³²SCP₂ did not potentiate the ability of SCP₂ to elicit intermembrane phospholipid transfer. The finding that ¹⁻³²SCP₂ potentiated the ability of SCP₂ to elicit intermembrane sterol transfer is also noteworthy in that earlier studies provided clues suggesting that the opposite might occur. For example, ¹⁻³²SCP₂ decreases/competes with SCP₂ for membrane binding (42). This would suggest that ¹⁻³²SCP₂ should inhibit rather than potentiate SCP₂-mediated intermembrane sterol transfer (43). On the contrary, the data showed that although ¹⁻³²SCP₂ peptide did not itself enhance sterol transfer, it potentiated the ability of SCP₂ to mediate intermembrane sterol transfer. Compared with SCP₂, addition of [SCP₂ + ¹⁻³²SCP₂] increased the initial rate of molecular sterol transfer nearly 3-fold (from 0.35 to 1.00 nmol/min) and reduced the half-time of the exchangeable pool 10-fold (from 11.6 to 1.2 min). While ¹⁻³²SCP₂ alone had no effect on either half-time or sterol domain size, SCP₂ alone decreased the half-time 4-fold and increased the exchangeable sterol domain size. The combination [SCP₂ + ¹⁻³²SCP₂] decreased the half-time an additional 10-fold, without further altering the size of the exchangeable sterol domain. Consequently, the effects of [SCP₂ + ¹⁻³²SCP₂] together were synergistic rather than simply additive.

Fourth, ¹⁻³²SCP₂ bound to anionic phospholipid-containing membranes to alter the physical properties of the membrane, including fluidity and sterol microenvironment. Decreased fluidity was shown by both ¹⁻³²SCP₂ and SCP₂ separately increasing the polarization of diphenylhexatriene, a probe of lipid fluidity, in anionic phospholipid-rich membranes. This effect was specific since diphenylhexatriene polarization and/or fluorescence intensity were not altered in neutral charged membranes and only slightly altered in aqueous buffer. Furthermore, [¹⁻³²SCP₂ + SCP₂] synergistically increased the polarization of diphenylhexatriene in anionic phospholipid-rich but not neutral charged membranes. These data suggest that ¹⁻³²SCP₂ and SCP₂ individually and synergistically altered the fluidity of the membrane. This observation is consistent with previous studies demonstrating that SCP₂ increased the surface pressure of monolayer model membranes (4). Altered sterol microenvironment was shown by the fact that addition of ¹⁻³²SCP₂ and SCP₂ to DHE-containing membranes increased both DHE lifetime components τ_1 and τ_2 by 11–15% and 44–84%, respectively. Increased lifetime is indicative of increased exposure of the

DHE to the aqueous environment and/or a change in the polarity of the membrane microenvironment wherein DHE resides (47). Thus, even though ¹⁻³²SCP₂ did not bind DHE, it altered the microenvironment of DHE in the membrane to increase the lifetime of DHE therein. Finally, these effects of ¹⁻³²SCP₂ and SCP₂ on binding to membranes and altering the structure of the membrane were not due to nonspecific disruption of the membrane. Neither ¹⁻³²SCP₂, SCP₂, nor modified SCP₂ N-terminal peptides significantly affected the permeability of the membrane to elicit leakage of small molecules. This may account for the ability of the ¹⁻³²SCP₂ peptide to facilitate the ability of SCP₂ to bind/extract the sterol from the membrane.

In summary, the data presented herein contribute significantly to our understanding of the mechanism whereby SCP₂ enhances intermembrane sterol transfer. The N-terminal amphipathic α -helix of SCP₂, comprised of amino acids 1–32 (i.e., ¹⁻³²SCP₂), is a membrane binding domain (42, 43). The results of this study showed for the first time that ¹⁻³²SCP₂ did not bind sterol in the membrane and did not itself elicit intermembrane sterol transfer. However, binding of ¹⁻³²SCP₂ to membranes did alter the structure of anionic phospholipid-containing membranes and the microenvironment wherein sterol was localized therein to make it more aqueous accessible. Therefore, ¹⁻³²SCP₂ potentiated the ability of SCP₂ to enhance intermembrane sterol transfer.

REFERENCES

- Gallegos, A. M., Atshaves, B. P., Storey, S. M., Starodub, O., Petrescu, A. D., Huang, H., McIntosh, A., Martin, G., Chao, H., Kier, A. B., and Schroeder, F. (2001) *Prog. Lipid Res.* 40, 498–563.
- Billheimer, J. T., Strehl, L. L., Davis, G. L., Strauss, J. F., III, and Davis, L. G. (1990) *DNA Cell Biol.* 9, 159–165.
- Wirtz, K. W., and Gadella, T. W., Jr. (1990) *Experientia* 46, 592–599.
- Van Amerongen, A., Demel, R. A., Westerman, J., and Wirtz, K. W. A. (1989) *Biochim. Biophys. Acta* 1004, 36–46.
- Billheimer, J. T., and Gaylor, J. L. (1990) *Biochim. Biophys. Acta* 1046, 136–143.
- Moncecchi, D. M., Nemezc, G., Schroeder, F., and Scallen, T. J. (1991) in *Physiology and Biochemistry of Sterols* (Patterson, G. W., and Nes, W. D., Eds.) pp 1–27, American Oil Chemists' Society Press, Champaign, IL.
- Schroeder, F., Jefferson, J. R., Kier, A. B., Knittell, J., Scallen, T. J., Wood, W. G., and Hapala, I. (1991) *Proc. Soc. Exp. Biol. Med.* 196, 235–252.
- Schroeder, F., Frolov, A. A., Murphy, E. J., Atshaves, B. P., Jefferson, J. R., Pu, L., Wood, W. G., Foxworth, W. B., and Kier, A. B. (1996) *Proc. Soc. Exp. Biol. Med.* 213, 150–177.
- Frolov, A. A., Woodford, J. K., Murphy, E. J., Billheimer, J. T., and Schroeder, F. (1996) *J. Lipid Res.* 37, 1862–1874.
- Frolov, A., Woodford, J. K., Murphy, E. J., Billheimer, J. T., and Schroeder, F. (1996) *J. Biol. Chem.* 271, 16075–16083.
- Schoer, J., Gallegos, A., Starodub, O., Petrescu, A., Roths, J. B., Kier, A. B., and Schroeder, F. (2000) *Biochemistry* 39, 7662–7677.
- Schroeder, F., Gallegos, A. M., Atshaves, B. P., Storey, S. M., McIntosh, A., Petrescu, A. D., Huang, H., Starodub, O., Chao, H., Yang, H., Frolov, A., and Kier, A. B. (2001) *Exp. Biol. Med.* 226, 873–890.
- Gallegos, A. M., Schoer, J., Starodub, O., Kier, A. B., Billheimer, J. T., and Schroeder, F. (2000) *Chem. Phys. Lipids* 105, 9–29.
- Atshaves, B. P., Starodub, O., McIntosh, A. L., Roths, J. B., Kier, A. B., and Schroeder, F. (2000) *J. Biol. Chem.* 275, 36852–36861.
- Moncecchi, D. M., Murphy, E. J., Prows, D. R., and Schroeder, F. (1996) *Biochim. Biophys. Acta* 1302, 110–116.
- Puglielli, L., Rigotti, A., Greco, A. V., Santos, M. J., and Nervi, F. (1995) *J. Biol. Chem.* 270, 18723–18726.
- Gallegos, A. M., Atshaves, B. P., Storey, S., McIntosh, A., Petrescu, A. D., and Schroeder, F. (2001) *Biochemistry* 40, 6493–6506.
- Murphy, E. J., and Schroeder, F. (1997) *Biochim. Biophys. Acta* 1345, 283–292.
- Seedorf, U., Raabe, M., Ellinghaus, P., Kannenberg, F., Fobker, M., Engel, T., Denis, S., Wouters, F., Wirtz, K. W. A., Wanders, R. J. A., Maeda, N., and Assmann, G. (1998) *Genes Dev.* 12, 1189–1201.
- Zanlungo, S., Amigo, L., Mendoza, H., Glick, J., Rodriguez, A., Kozarsky, K., Miquel, J. F., Rigotti, A., and Nervi, F. (2000) *Gastroenterology* 118, 135 (Abstract 1165).
- Kawata, S., Imai, Y., Inada, M., Inui, M., Kakimoto, H., Fukuda, K., Maeda, Y., and Tarui, S. (1991) *Clin. Chim. Acta* 197, 201–208.
- Hafer, A., Katzberg, N., Muench, C., Scheibner, J., Stange, E. F., Seedorf, U., and Fuchs, M. (2000) *Gastroenterology* 118, 135.
- Keller, G. A., Scallen, T. J., Clarke, D., Maher, P. A., Krisans, S. K., and Singer, S. J. (1989) *J. Cell Biol.* 108, 1353–1361.
- Schroeder, F., Frolov, A., Schoer, J., Gallegos, A., Atshaves, B. P., Stolowich, N. J., Scott, A. I., and Kier, A. B. (1998) in *Intracellular Cholesterol Trafficking* (Chang, T. Y., and Freeman, D. A., Eds.) pp 213–234, Kluwer Academic Publishers, Boston.
- Atshaves, B. P., Petrescu, A., Starodub, O., Roths, J., Kier, A. B., and Schroeder, F. (1999) *J. Lipid Res.* 40, 610–622.
- Starodub, O., Jolly, C. A., Atshaves, B. P., Roths, J. B., Murphy, E. J., Kier, A. B., and Schroeder, F. (2000) *Am. J. Physiol.* 279, C1259–C1269.
- Schroeder, F., Frolov, A., Starodub, O., Russell, W., Atshaves, B. P., Petrescu, A. D., Huang, H., Gallegos, A., McIntosh, A., Tahotna, D., Russell, D., Billheimer, J. T., Baum, C. L., and Kier, A. B. (2000) *J. Biol. Chem.* 275, 25547–25555.
- Gadella, T. W. J., Bastiaens, P. I. H., Visser, A. J. W. G., and Wirtz, K. W. A. (1991) *Biochemistry* 30, 5555–5564.
- Schroeder, F., Butko, P., Nemezc, G., and Scallen, T. J. (1990) *J. Biol. Chem.* 265, 151–157.
- Colles, S. M., Woodford, J. K., Moncecchi, D., Myers-Payne, S. C., McLean, L. R., Billheimer, J. T., and Schroeder, F. (1995) *Lipids* 30, 795–804.
- Seedorf, U., Scheek, S., Engel, T., Steif, C., Hinz, H. J., and Assmann, G. (1994) *J. Biol. Chem.* 269, 2613–2618.
- Stolowich, N. J., Frolov, A., Atshaves, B. P., Murphy, E., Jolly, C. A., Billheimer, J. T., Scott, A. I., and Schroeder, F. (1997) *Biochemistry* 36, 1719–1729.
- Jatzke, C., Hinz, H. J., Seedorf, U., and Assmann, G. (1999) *Biochim. Biophys. Acta* 1432, 265–274.
- Szyperski, T., Scheek, S., Johansson, J., Assmann, G., Seedorf, U., and Wuthrich, K. (1993) *FEBS Lett.* 335, 18–26.
- Weber, F. E., Dyer, J. H., Garcia, F. L., Werder, M., Szyperski, T., Wuthrich, K., and Hauser, H. (1998) *Cell. Mol. Life Sci.* 54, 751–759.
- Stolowich, N. J., Frolov, A., Petrescu, A. D., Scott, A. I., Billheimer, J. T., and Schroeder, F. (1999) *J. Biol. Chem.* 274, 35425–35433.
- Garcia, F. L., Szyperski, T., Dyer, J. H., Choinowski, T., Seedorf, U., Hauser, H., and Wuthrich, K. (2000) *J. Mol. Biol.* 295, 595–603.
- Stolowich, N. J., Petrescu, A. D., Huang, H., Martin, G., Scott, A. I., and Schroeder, F. (2002) *Cell. Mol. Life Sci.* 59, 193–212.
- Choinowski, T., Dyer, J. H., Maderegger, B., Winterhalter, K. M., Hauser, H., and Piotnek, K. (1999) *Acta Crystallogr. D55*, 1478–1480.
- Choinowski, T., Hauser, H., and Piotnek, K. (2000) *Biochemistry* 39, 1897–1902.
- Woodford, J. K., Colles, S. M., Myers-Payne, S., Billheimer, J. T., and Schroeder, F. (1995) *Chem. Phys. Lipids* 76, 73–84.
- Huang, H., Ball, J. A., Billheimer, J. T., and Schroeder, F. (1999) *Biochem. J.* 344, 593–603.
- Huang, H., Ball, J. A., Billheimer, J. T., and Schroeder, F. (1999) *Biochemistry* 38, 13231–13243.
- Matsuura, J. E., George, H. J., Ramachandran, N., Alvarez, J. G., Strauss, J. F. I., and Billheimer, J. T. (1993) *Biochemistry* 32, 567–572.
- Schroeder, F., Barenholz, Y., Gratton, E., and Thompson, T. E. (1987) *Biochemistry* 26, 2441–2448.
- Hapala, I., Kavecansky, J., Butko, P., Scallen, T. J., Joiner, C., and Schroeder, F. (1994) *Biochemistry* 33, 7682–7690.
- Nemezc, G., and Schroeder, F. (1988) *Biochemistry* 27, 7740–7749.

48. Nemezc, G., Fontaine, R. N., and Schroeder, F. (1988) *Biochim. Biophys. Acta* 943, 511–521.
49. Butko, P., Hapala, I., Nemezc, G., and Schroeder, F. (1992) *J. Biochem. Biophys. Methods* 24, 15–37.
50. Ladokhin, A. S., Wimley, W. C., and White, S. H. (1995) *Biophys. J.* 69, 1964–1971.
51. Ladokhin, A. S., Selsted, M. E., and White, S. H. (1997) *Biophys. J.* 72, 794–805.
52. Wimley, W. C., Selsted, M. E., and White, S. H. (1994) *Protein Sci.* 3, 1362–1373.
53. Incerpi, S., Jefferson, J. R., Wood, W. G., Ball, W. J., and Schroeder, F. (1992) *Arch. Biochem. Biophys.* 298, 35–42.
54. Woodford, J. K., Jefferson, J. R., Wood, W. G., Hubbell, T., and Schroeder, F. (1993) *Biochim. Biophys. Acta* 1145, 257–265.
55. Schroeder, F., Colles, S. M., Kreishman, G. P., Heyliger, C. E., and Wood, W. G. (1994) *Arch. Biochem. Biophys.* 309, 369–376.
56. Colles, S. M., Wood, W. G., Myers-Payne, S. C., Igbavboa, U., Avdulov, N. A., Joseph, J., and Schroeder, F. (1995) *Biochemistry* 34, 5945–5959.
57. Schroeder, F., Myers-Payne, S. C., Billheimer, J. T., and Wood, W. G. (1995) *Biochemistry* 34, 11919–11927.
58. Frolov, A., Cho, T. H., Murphy, E. J., and Schroeder, F. (1997) *Biochemistry* 36, 6545–6555.
59. Thoma, S., Kaneko, Y., and Somerville, C. (1993) *Plant J.* 3, 427–436.
60. Hapala, I., Butko, P., and Schroeder, F. (1990) *Chem. Phys. Lipids* 56, 37–47.
61. Ito, T., Kawata, S., Imai, Y., Kakimoto, H., Trzaskos, J., and Matsuzawa, Y. (1996) *Gastroenterology* 110, 1619–1627.
62. Fuchs, M., Lammert, F., Wang, D. Q. H., Paigen, B., Carey, M. C., and Cohen, D. E. (1998) *Biochem. J.* 336, 33–37.
63. Schroeder, F., Butko, P., Hapala, I., and Scallen, T. J. (1990) *Lipids* 25, 669–674.
64. Butko, P., Hapala, I., Scallen, T. J., and Schroeder, F. (1990) *Biochemistry* 29, 4070–4077.
65. Gadella, T. W., Jr., and Wirtz, K. W. (1991) *Biochim. Biophys. Acta* 1070, 237–245.

BI0260536